



A General Biphasic Bodyweight Model for Scaling Basal Metabolic Rate, Glomerular Filtration Rate, and Drug Clearance from Birth to Adulthood

Teh-Min Hu¹

Received: 1 March 2022 / Accepted: 26 April 2022 / Published online: 10 May 2022
© The Author(s), under exclusive licence to American Association of Pharmaceutical Scientists 2022

Abstract

The objective of this study is to propose a unified, continuous, and bodyweight-only equation to quantify the changes of human basal metabolic rate (*BMR*), glomerular filtration rate (*GFR*), and drug clearance (*CL*) from infancy to adulthood. The *BMR* datasets were retrieved from a comprehensive historical database of male and female subjects (0.02 to 64 years). The *CL* datasets for 17 drugs and the *GFR* dataset were generated from published maturation and growth models with reported parameter values. A statistical approach was used to simulate the model-generated *CL* and *GFR* data for a hypothetical population with 26 age groups (from 0 to 20 years). A biphasic equation with two power-law functions of bodyweight was proposed and evaluated as a general model using nonlinear regression and dimensionless analysis. All datasets universally reveal biphasic curves with two distinct linear segments on log–log plots. The biphasic equation consists of two reciprocal allometric terms that asymptotically determine the overall curvature. The fitting results show a superlinear scaling phase (asymptotic exponent >1 ; ca. 1.5–3.5) and a sublinear scaling phase (asymptotic exponent <1 ; ca. 0.5–0.7), which are separated at the phase transition bodyweight ranging from 5 to 20 kg with a mean value of 10 kg (corresponding to 1 year of age). The dimensionless analysis generalizes and offers quantitative realization of the maturation and growth process. In conclusion, the proposed mixed-allometry equation is a generic model that quantitatively describes the phase transition in the human maturation process of diverse human functions.

KEY WORDS allometry · drug clearance · basal metabolic rate · glomerular filtration rate · maturation and growth

INTRODUCTION

Human metabolic processes undergo continuous changes during the growth and maturation stages (1, 2). It is generally accepted that human physiological and metabolic parameters (*Y*) do not scale linearly with bodyweight (*W*) but scale with a power-law function, in the form of $Y = aW^b$, where *a* and *b* are constants. This simple allometric equation is linear in a double logarithmic plot (i.e., log *Y* vs. log *W*), which has been used to describe datasets of basal metabolic rate (*BMR*), glomerular filtration rate (*GFR*), and drug clearance (*CL*) (3, 4). However, if data from neonates and

adults were pooled for analysis, the resulting plots are usually curved with a steeper early phase, followed by a shallower later phase (3, 5–7). Accordingly, simple allometry with a fixed exponent, or with a specific exponent obtained from the adult data, would systematically overestimate *GFR* or *CL* values among the youngest (3, 7, 8). In the biology field, extensive studies have shown that the metabolic pace of animals or plants shifts at certain points of organism's life; such shifting exhibits multiple linear phases connected at one or more transitional points in log–log size-scaling plots (9–13). The metabolic shifting phenomenon has long been recognized in human (5), and the quest for a general quantitative model has never ceased (8, 14–17). Thus, the current study addresses the feasibility of using one unified, empirical equation, where bodyweight is the only independent variable, to quantitatively describe the maturation of human physiological and metabolic functions.

The basal metabolic rate (*BMR*), i.e., the rate of energy transformation within the body at rest, is perhaps the most

✉ Teh-Min Hu
tehmin@nycu.edu.tw

¹ Department of Pharmacy, School of Pharmaceutical Sciences, National Yang Ming Chiao Tung University, Taipei 112, Taiwan

fundamental biological rate. *BMR* is considered as a universal “pacemaker” for biological processes (11). Therefore, allometric scaling of *BMR* has gained much attention and been hotly debated for over a century. In biology, the discussion has been shifted from whether there is a universal scaling law to how intra- and interspecific scaling vary beyond the “3/4-power” law (10). In medicine, human energy requirements are important considerations in clinical and public health nutrition (4, 18–22). Thus, the WHO issues sex- and age-specific recommendations on human energy requirements (23). The WHO recommendations consist, for each sex, of 3 bodyweight-based linear equations for estimating *BMR*. The equations have different constant values for separate age groups (0–3 years, 4–10 years, and 11–18 years), suggesting that *BMR* varies with bodyweight in a nonlinear manner during the growth period. To date, the inherent nonlinearity in human metabolic scaling remains to be addressed by a unified quantitative model.

Glomerular filtration rate (*GFR*) is an important parameter of renal function. In pharmacology and toxicology, *GFR* determines the renal elimination capacity for xenobiotics and environmental toxicants. The information of *GFR* is particularly useful for dosing renally cleared drugs, especially for pediatric patients, because dosing information for children is often limited by ethical and clinical considerations in clinical trials. Accordingly, attempts have been made to predict pediatric *GFR* values from adult’s value using quantitative models (7). Existing data show that *GFR* undergoes continuous change after birth and reaches adult’s level in the early childhood (7, 24). Several models have been proposed to model the growth and maturation of *GFR*, with a focus on predicting *GFR* for neonates or children from adults (6, 7). The previous models have different levels of complexity. The simplest model has the form of simple allometry, where *GFR* scales with bodyweight in a single power-law function, with either fixed or variable exponents (6). More complicated models include both age and bodyweight as the input variables (7, 24). The prediction models are useful for predicting population mean values but not for individual prediction (6).

Drug clearance (*CL*) is an essential pharmacokinetic parameter that offers direct estimation of drug dose. The acquisition of accurate *CL* information is critical in drug development and in drug therapy. However, the pediatric *CL* data are less attainable, because of the limitation of conducting clinical trials in young subjects. Thus, various prediction models have been proposed to draw quantitative relationship between *CL* and age and/or bodyweight (3, 8, 25–27). The magnitude of *CL* is correlated with body size and determined by the function of drug elimination organs (i.e., the kidneys and liver). Therefore, *CL* values are subjected to changes of renal and hepatic functions during maturation and growth. The *CL* values of many drugs have been

compiled from both population pharmacokinetic studies and physiologically based pharmacokinetic (PBPK) modeling (8, 28–32). Besides, several growth and maturation models have been evaluated for their predictive performance (17, 30, 33–35). Overall, the previous findings are highlighted as follows: first, *CL* scales with bodyweight raised to a power that is variable with age or body weight (16, 28, 30). Second, more profound changes were observed in earlier life than in later life (e.g., neonates to toddlers vs. toddlers to adolescents or adults) (28, 30). Finally, a quantitative birth-to-adulthood model usually includes both age and bodyweight as the independent variables (7, 8, 15, 31, 36, 37), although, for some drugs and in particular age groups, e.g., in younger aged children, clearance can be scaled with bodyweight alone (3, 8, 30, 38–40).

Taken together, human *BMR*, *GFR*, and *CL* values seemed to share similar rate-switching features during the human maturation and growth processes. The aim of this study is to evaluate a continuous, single, bodyweight-only equation for its potential as a unified empirical model for scaling human *BMR*, *GFR*, and *CL* from neonates to adults. The equation is in the form of reciprocal sum of two power-law functions of bodyweight with 4 parameters (so-called mixed-allometry or mixed-power-law equation). All the datasets evaluated in this study were either directly retrieved from the literature or generated from existing age- and bodyweight equations with published parameters. The datasets thus represent the tendency of each specific dependent variable of interest (*BMR*, *GFR*, or *CL*), and the overall goal is not to predict the unknown, but to infer common quantitative understanding from analysis of diverse datasets.

METHODS

BMR Datasets

The basal metabolic rate (*BMR*) data, in kcal/day, for males and females from birth to adulthood were obtained from the historical database compiled by Schofield (41). The *BMR* data in MJ/day was converted to kcal/day. The database included *BMR* data for 4811 males (0.02–52.3 years, 2.7–108.9 kg) and 2364 females (0.14–64 years, 2.0–96.4 kg). The data are listed according to divided bodyweight groups (separated by 1 kg up to ~100 kg). The majority of groups contain >5 subjects (up to 189 subjects).

GFR Dataset

The glomerular filtration rate (*GFR*) data, in mL/min, were generated using the general equation proposed by the research group of Anderson (24, 37, 42) for hypothetical human subjects:

$$P = P_{adult} \cdot F_{age} \cdot F_{size} \tag{1}$$

where here P is GFR and P_{adult} is the adult GFR value (136 mL/min (7)), F_{age} is the age function (maturation function), and F_{size} is the body size function (allometric function):

$$F_{age} = \frac{PMA^\theta}{(TM_{50})^\theta + PMA^\theta} \tag{2}$$

$$F_{size} = \left(\frac{W}{W_{adult}}\right)^\mu \tag{3}$$

The variables and parameters are defined as PMA , postmenstrual age (weeks); θ , the Hill coefficient; TM_{50} , maturation half-life; W , bodyweight of the individual; W_{adult} , adult bodyweight (70 kg); and μ , allometric, bodyweight exponent.

The GFR dataset was generated for a hypothetical population from 0 to 20 years of postnatal age. The age–bodyweight information was mainly obtained from Annex 2 in ref. (43). Additional age–bodyweight data for infants < 0.25 years were retrieved from ref. (7). A total of 26 age groups were included for the simulation: 0, 0.083, 0.167, 0.25, 0.5, 0.75, 1, 1.5, 2, 3, 4, 5, 6, 7, 8, 9, 10, 11, 12, 13, 14, 15, 16, 17, 18, and 20 years. The mean bodyweight for each age group was either directly retrieved from the reported mean values (7) or estimated from the reported median values (43). Assuming lognormal distribution (44, 45), the median (μ^*) was transformed to mean (μ) using the following formula (46): $\mu = \ln \mu^*$. The standard deviation (σ) of lognormal distribution was estimated as $\sigma = \sqrt{\ln(CV^2 + 1)}$, where CV is the arithmetic coefficient of variation (47). For each age group, the bodyweight was randomly generated using the age-specific μ and σ , assuming $CV = 0.15$ in a population (43). This sampling process was conducted using the built-in functions, *RandomVariate* and *LogNormalDistribution*, in Mathematica®. The postmenstrual ages (PMA) were calculated by adding a gestational age of 40 weeks (24) to the postnatal ages. The resulting (PMA , W) data were plugged into Equations 1–3 to generate expected GFR values, using the reported parameter values (24): $\theta = 3.4$, $TM_{50} = 47.7$ weeks, $\mu = 0.75$. To add variability to the GFR values, the lognormal distribution was assumed with $CV = 0.2$. For each age group, GFR values for 20 randomly selected subjects were simulated. The data for 26 age groups (a total of 520 data points) were pooled as the GFR dataset

Drug CL Datasets

The first CL datasets were retrieved from Björkman’s work (29) on physiologically based pharmacokinetic ($PBPK$) modeling for two drugs, theophylline and midazolam. The

CL and bodyweight values of both sexes are directly available for neonates; children ages 0.5, 1, 2, 5, 10, and 15 years; and adults. The total CL values were estimated from $PBPK$ -modeled hepatic CL and/or renal CL (if applicable). These CL datasets were evaluated in the initial modeling trial for drug CL .

Next, the extended modeling was applied to CL datasets of 17 drugs, which have been previously modeled using the growth and maturation model of Anderson *et al.* (15, 37, 42); the model parameters were directly available from the literature (15). The CL values were generated using the same general models, as described in Equations 1–3, where P and P_{adult} are replaced by CL and CL_{adult} . All the drug-specific parameters in the age function (Equation 2) and size function (Equation 3) were taken from the literature (15). For each drug, the CL values with random errors were generated for 26 age groups (each of 20 subjects). The procedure to generate the CL values with random errors was the same as that described above for GFR .

Finally, individual experimental data were retrieved from two pharmacokinetic studies of cefetamet in pediatric patients (48, 49). The first study included 20 infants of 0.19 to 1.44 years (48). The second study included 18 children (3 to 12 years). The adult data (50, 51) were also included to complete the cefetamet dataset.

Model Fitting and Validation

In this study, the following mixed-power equation was proposed to model the datasets mentioned above.

$$\frac{1}{P} = \frac{1}{A \cdot W^\alpha} + \frac{1}{B \cdot W^\beta} \tag{4}$$

or

$$P = \left(\frac{1}{A \cdot W^\alpha} + \frac{1}{B \cdot W^\beta}\right)^{-1} \tag{5}$$

where P is the metabolic or physiological quantity of interest, viz., BMR , GFR , or drug CL . The equation consists of two allometric coefficients ($0 < A < B$) and two allometric exponents ($\alpha > \beta > 0$). For model comparison, the simple allometric model was also included for analysis:

$$P = GW^\gamma \tag{6}$$

where G and γ are the allometric coefficient and exponent, respectively.

Model fitting was performed using the nonlinear regression function (*NonlinearModelFit*) in Mathematica® (Wolfram). The model parameters were obtained by fitting the model equations to all available datasets (with suitable weighting functions, e.g., $1/y^2$). The comparison of the biphasic allometry (BA) model with the simple allometry

(SA) model was based on the Akaike’s information criterion (AIC). Besides, the model fitting was validated using multiple measures, including residual plots, R^2 , and t statistic for the fitted parameters.

Estimation of the Characteristic Values

The biphasic model is characterized by continuous change of slope in the $\log P$ vs. $\log W$ plot. The weight-dependent slope (S) of the fitted biphasic curve was generated using the following equation (see Appendix for the derivation):

$$S = \alpha \left(\frac{B \cdot W^\beta}{A \cdot W^\alpha + B \cdot W^\beta} \right) + \beta \left(\frac{A \cdot W^\alpha}{A \cdot W^\alpha + B \cdot W^\beta} \right) \quad (7)$$

The biphasic growth and maturation curve switches at a characteristic bodyweight (i.e., the bodyweight at the phase transition, \tilde{w}), which was calculated using the following expression (Appendix).

$$\tilde{w} = (B/A)^{1/(\alpha-\beta)} \quad (8)$$

The characteristic slope (S^*) at the phase transition bodyweight was calculated as the sum of the allometric exponents (Appendix), i.e.,

$$S^* = (\alpha + \beta)/2 \quad (9)$$

Dimensionless Analysis

To conduct a dimensionless analysis, Equation 4 is treated as follows. First, let $X = W/\tilde{w}$, where W is the exact bodyweight and \tilde{w} represents the critical bodyweight at the phase transition. Thus, X is the dimensionless, fractional number associated with bodyweight. Similarly, let $Y = P/\tilde{p}$, where P is physiological parameters such as BMR and GFR or CL and \tilde{p} is the corresponding P value at $W = \tilde{w}$, and according to Equation 4,

$$\frac{1}{\tilde{p}} = \frac{1}{A\tilde{w}^\alpha} + \frac{1}{B\tilde{w}^\beta} \quad (10)$$

Accordingly, Y is defined as the fractional value of BMR , GFR , or CL (relative to their critical value at phase transition). Then, the original Equation 4 can be expressed and rearranged as follows:

$$\frac{1}{\tilde{p}Y} = \frac{1}{A(\tilde{w}X)^\alpha} + \frac{1}{B(\tilde{w}X)^\beta} \quad (11)$$

$$\frac{1}{Y} = \tilde{p} \left(\frac{1}{A(\tilde{w}X)^\alpha} + \frac{1}{B(\tilde{w}X)^\beta} \right) \quad (12)$$

By substituting \tilde{p} in the last equation from Equation 10, and after further rearrangement, the final equation is obtained:

$$\frac{1}{Y} = f_1 \left(\frac{1}{X^\alpha} \right) + f_2 \left(\frac{1}{X^\beta} \right) \quad (13)$$

Where

$$f_1 = \frac{B\tilde{w}^\beta}{A\tilde{w}^\alpha + B\tilde{w}^\beta} = \frac{1}{2} \quad (14)$$

$$f_2 = \frac{A\tilde{w}^\alpha}{A\tilde{w}^\alpha + B\tilde{w}^\beta} = \frac{1}{2} \quad (15)$$

Accordingly,

$$Y = 2 \left(\frac{X^\alpha \cdot X^\beta}{X^\alpha + X^\beta} \right) \quad (16)$$

The slope of the dimensionless biphasic-scaling curves (on a log–log plot) has the following form:

$$slope = \frac{d \ln Y}{d \ln X} = \alpha \left(\frac{X^\beta}{X^\alpha + X^\beta} \right) + \beta \left(\frac{X^\alpha}{X^\alpha + X^\beta} \right) \quad (17)$$

At $X \ll 1$, the slope is approaching the asymptotic exponent, α , whereas at the other end (i.e., $X \gg 1$) the slope is approaching another exponent, β . Since $\alpha > \beta$, the slope continuously decreases as X increases. Thus, the decrease of slope (or “deceleration”) is expressed as

$$deceleration = \frac{dslope}{d \ln X} = -(\alpha - \beta)^2 \left(\frac{X^\alpha}{X^\alpha + X^\beta} \right) \left(\frac{X^\beta}{X^\alpha + X^\beta} \right) \quad (18)$$

The deceleration equation—which always gives a negative value—quantifies the change (i.e., continuous slowing down) of pace in the growth and maturation process. In this study, different physiological and clearance datasets were harmonized using the derived dimensionless equations and the fitted parameter values for various datasets. Specifically, the dimensionless Y values were simulated using Equation 13 with input X values ranging from 0.1 to 10 (step of increment = 0.1). The corresponding slope and deceleration curves were generated using Equation 17 and Equation 18, respectively.

Fig. 1. Bodyweight scaling of *BMR* datasets. *BMR* data were retrieved from Schofield’s historical database (41). **A** Comparison of model fittings for the male dataset. Solid line, biphasic model (Equation 4); dashed line, simple allometry model (Equation 6). **B** Comparison of model fittings for the female dataset. **C** The residual plots for the male data. Solid symbol, biphasic model; open symbol, simple allometry. **D** The residual plots for the female data

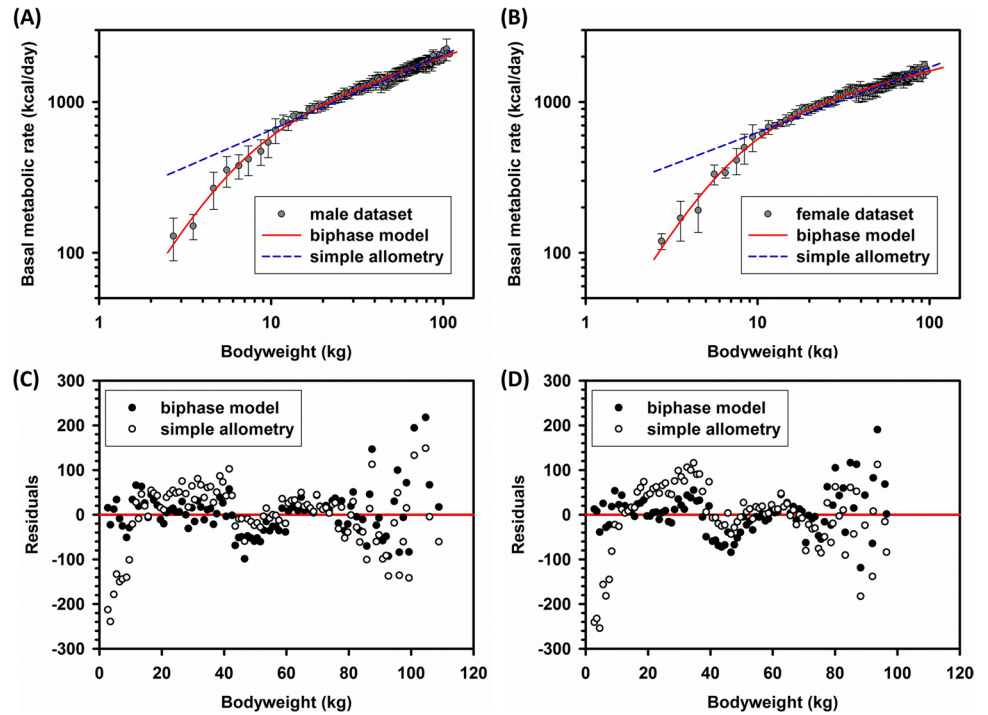


Table I Model Fitting Results for Basal Metabolic Rate

	<i>A</i>	α	<i>B</i>	β	\tilde{w}	<i>S</i> *	<i>AIC</i> (<i>BA</i> , <i>SA</i>)
Male	19.5 ± 2.5	2.04 ± 0.11	327 ± 26	0.39 ± 0.02	5.52	1.22	(1092, 1151)
Female	17.3 ± 2.3	2.00 ± 0.10	444 ± 44	0.28 ± 0.02	6.64	1.14	(983, 1063)

The model parameter estimates (± SE) include the allometric parameters (*A*, *B*) and bodyweight exponents (α , β), according to Equation 4; bodyweight at phase transition, $w = (B/A)^{1/(\alpha-\beta)}$ (Equation 8); the slope at transition, $S^* = (\alpha + \beta)/2$ (Equation 9); Akaike’s information criterion (*AIC*); biphasic allometry model (*BA*); simple allometry model (*SA*). The parameter estimates for *SA* (Equation 6) are *G* = 209 (male) and 232 (female); γ = 0.50 (male) and 0.43 (female)

RESULTS

Scaling Basal Metabolic Rate

The biphasic allometry (*BA*) model and the simple allometry (*SA*) model were fitted to the Schofield’s historical dataset of *BMR* (41). Figure 1 shows the fitting results for the male and female datasets. The log *BMR* vs. log *W* plot (Fig. 1A and B) reveals curvature with two obvious phases. Thus, the mixed-power equation (the biphasic model) offers better fitting results with smaller *AIC* values than the simple allometry equation (Table I; Fig. 1A and B). Particularly, the *SA* model systematically overestimates the *BMR* values at *W* < 10 kg but underestimates the values at the *W* range of 10 to 40 kg (Fig. 1C and D). The slope of the biphasic curve decreases with increasing bodyweight; at the extreme body sizes, the slope approaches the two asymptotic allometric exponents, α and β (Fig. 2). The first exponent is about 2, whereas the

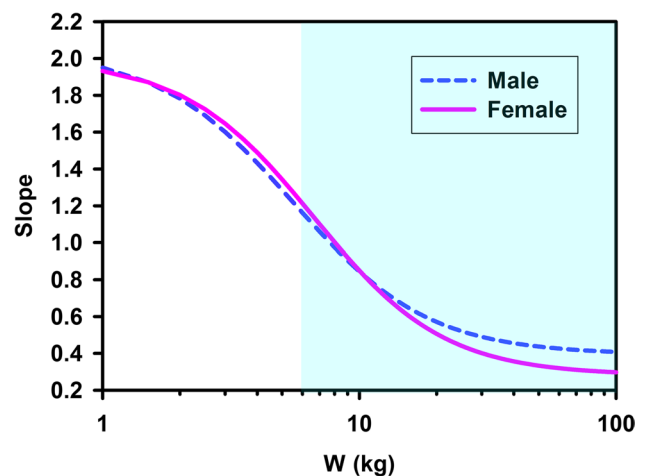


Fig. 2. The slope plots for the biphasic model. The changes of the slope on the log–log biphasic plots of the *BMR* datasets were quantified using Equation 7. The slopes for the males (dashed line) and females (solid line) have a sharp turnaround around 6 kg. The shaded area highlights the transition of the two phases

second exponent is near 0.3 or 0.4 (Table I). Accordingly, the first phase has a superlinear scaling relationship (slope >1), whereas the second phase scales sublinearly (slope <1). The two phases have a characteristic transition point at 5.5 kg and 6.6 kg, for males and females, respectively (Table I). Figure 2 highlights the phase transition as the body grows. The slope at the phase transition is the mean of the two asymptotic exponents (Equation 9) (male, 1.22, and female, 1.14).

Scaling the Glomerular Filtration Rate (GFR)

To demonstrate whether the proposed biphasic model could also be applied for scaling *GFR*, the (*GFR*, *W*) data were simulated for a hypothetical population with 26 age groups. In each group, the bodyweight for 20 subjects was randomly sampled from a lognormal distribution with transformed population mean and estimated standard deviation. The *GFR* values with random errors ($CV = 20\%$) were generated according to Equations 1–3 and using reported parameter values (24), assuming lognormal distribution. The data of all age groups were pooled and then fitted to the biphasic mixed-power equation. Figure 3 shows again a biphasic log–log profiles. The fitted parameter values are $A = 0.38 \pm 0.07$, $\alpha = 2.18 \pm 0.15$, $B = 14.0 \pm 3.5$, $\beta = 0.50 \pm 0.06$. The result is consistent with a superlinear scaling phase (slope >1) and a sublinear scaling phase (slope <1). The scaling slope decreases with increasing bodyweight (Fig. 3A). The phase transition occurs at 8.6 kg, and the slope at the transition is 1.34. The simple allometry model overestimates *GFR*, again, at $W < 10$ kg (Fig. 3B and D). Overall, the biphasic

model provides better fit with lower *AIC* (3774 vs. 4294) and more randomly scattered residuals (Fig. 3C).

Scaling Drug Clearance

Three types of drug clearance data were included for analysis. First, the proposed biphasic model was fitted to the cross-age *CL* data for theophylline (Fig. 4A and B) and midazolam (Fig. 4C and D), which were taken directly from a *PBPK* modeling study (29). The datapoints are scarcely distributed in the bodyweight range spanning neonates and adults. Nevertheless, compared with simple allometry (based on *AIC* and residual plots), the biphasic allometry model provides better fitting results (Table II). Again, the features of the biphasic model (i.e., 2 phases with defined phase transition) were clearly illustrated in this analysis. The two drugs have high first-phase exponents (ca. 2.6 to 3) and comparable—but less than unity—second-phase exponents (ca. 0.5 to 0.6). The results also show superlinear allometry in the early childhood and sublinear allometry in the later life. The transition occurs at 8.6 to 9.5 kg, with the corresponding slope values (S^*) close to 1.6 and 1.8, for theophylline and midazolam, respectively (Table II).

Secondly, the analysis was extended to 17 drugs whose ontogeny *CL* data have been previously modeled using the sigmoid *Emax* maturation model. All the model parameters, including the maturation half-life (TM_{50}) and the slope (Hill) coefficient, were summarized in the review article of Holford, Heo, and Anderson (15). To generate the ontogeny *CL* values for each drug, the drug-specific parameters were directly retrieved and plugged into the growth and

Fig. 3. Bodyweight scaling of model simulated *GFR*. *GFR* values with random errors (symbol) for 26 age groups (20 datapoints for each group) were simulated using the growth and maturation model of Andersen *et al.* (Equations 1–3). **A** The log–log plot for (*GFR*, *W*) and the slope plot. The solid line represents the nonlinear best-fit for the biphasic model (Equation 4). The dashed line is a weight-dependent slope of the fitted curve (Equation 7). **B** The residual plot for the biphasic model. **C** The same data were fitted to the simple allometry model (Equation 6). **D** The residual plot for the simple allometry model

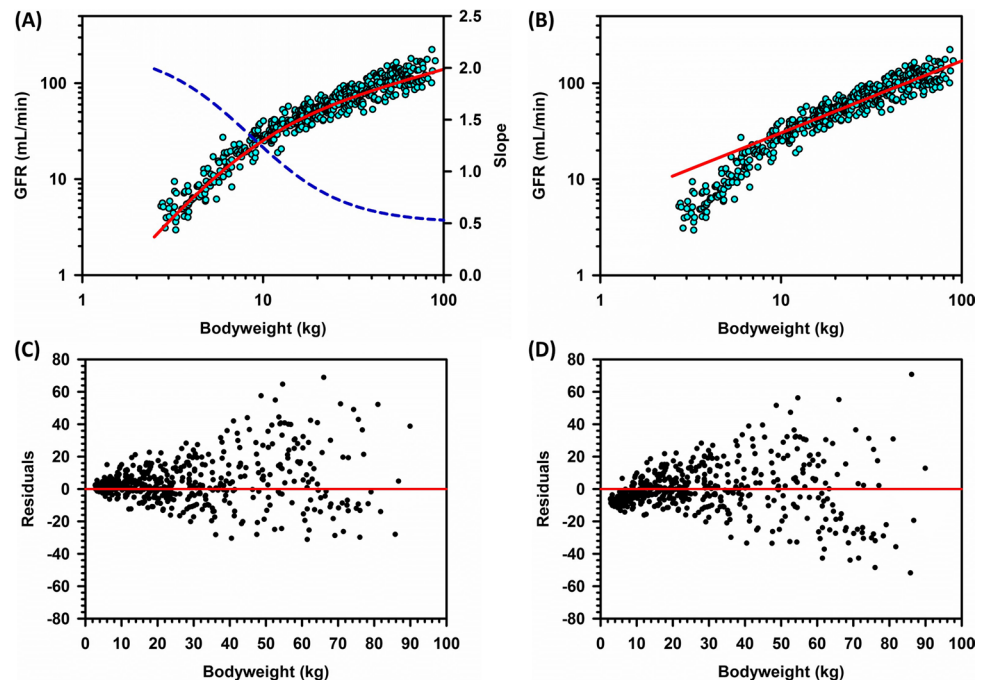


Fig. 4. Bodyweight scaling of drug clearance. The log *CL* vs. log *W* plots and the slope plots for theophylline (A and B) and midazolam *CL* (C and D). Symbols are *PBPK*-modeled *CL* values directly taken from the literature (29). Lines are the best nonlinear regression fits for the biphasic model

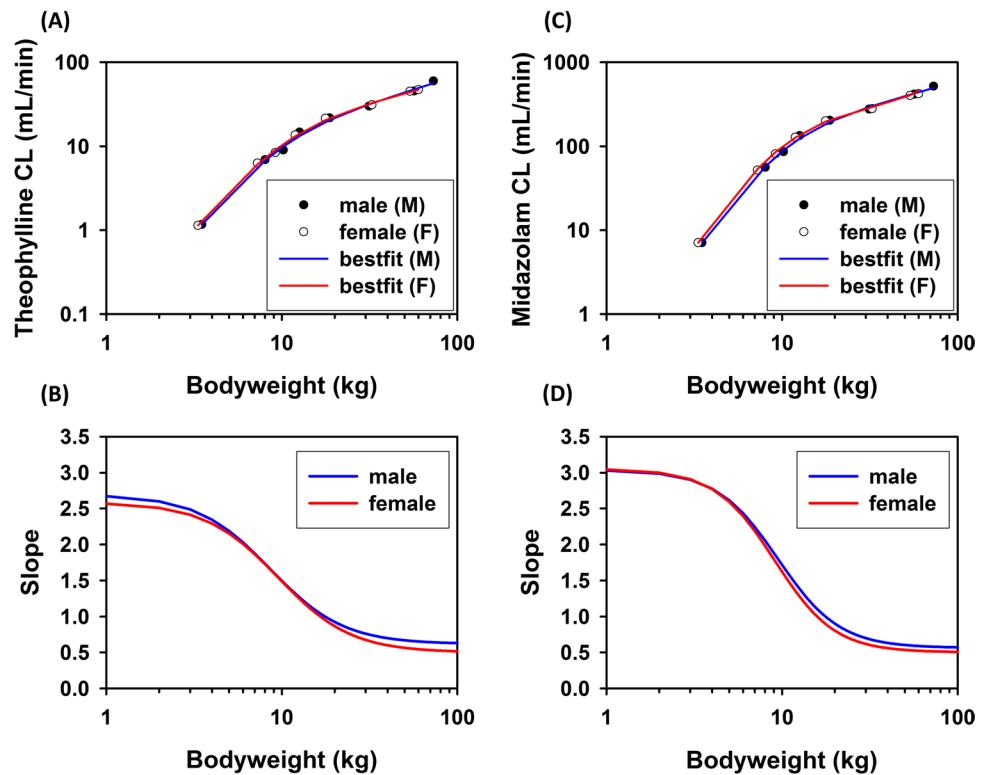


Table II Model Fitting Results for Theophylline and Midazolam Clearance

	<i>A</i>	α	<i>B</i>	β	\tilde{w}	<i>S</i> *	<i>AIC</i> (<i>BA</i> , <i>SA</i>)
Theophylline							
Male	0.05 ± 0.02	2.70 ± 0.39	4.03 ± 2.69	0.62 ± 0.16	8.60	1.66	(33.0, 41.5)
Female	0.06 ± 0.02	2.59 ± 0.22	6.18 ± 3.16	0.50 ± 0.13	9.50	1.55	(25.3, 41.9)
Midazolam							
Male	0.17 ± 0.05	3.04 ± 0.21	44.3 ± 17.1	0.56 ± 0.10	9.47	1.80	(62.1, 78.5)
Female	0.19 ± 0.04	3.05 ± 0.14	53.8 ± 14.7	0.50 ± 0.07	9.09	1.78	(55.0, 78.8)

PBPK-modeled *CL* data were retrieved from ref. (29). The model parameter estimates (± SE) include the allometric parameters (*A*, *B*) and bodyweight exponents (α , β), according to Equation 4; bodyweight at phase transition, $w = (B/A)^{1/(\alpha-\beta)}$ (Equation 8); the slope at transition, $S^* = (\alpha + \beta)/2$ (Equation 9); Akaike’s information criterion (*AIC*); biphasic allometry model (*BA*); simple allometry model (*SA*).

The parameter estimates for *SA* (Equation 6) are for theophylline, *G* = 1.50 (male) and 1.67 (female); γ = 0.85 (male) and 0.82 (female); for midazolam, *G* = 14.9 (male) and 15.9 (female); γ = 0.83 (male) and 0.81 (female).

maturation model (i.e., Equations 1–3, where the variable *P* is *CL*). Specifically, the *CL* values with random errors for 26 age groups (20 subjects/group) were simulated using the same approach described for the *GFR* dataset. For each drug, the population pooled (*CL*, *W*) data were then fitted to the biphasic model (Equation 4) and the simple allometry model (Equation 6). Note that the model used for generating the *CL* datasets is independent of the biphasic model used for model fitting.

The 17 drugs belong to 8 therapeutic categories, including antiviral agents (acyclovir, lamivudine, penciclovir), antineoplastic agents (busulfan), anticonvulsants

(levetiracetam), analgesics (acetaminophen, morphine, valdecoxib), anesthetics (dexmedetomidine, levobupivacaine, propofol, midazolam, ropivacaine), antibacterial agents (vancomycin), anti-ulcer agents (pantoprazole), and anti-malarials (pyrimethamine, sulfadoxine). The pharmacokinetic properties are diverse, covering drugs that are either mainly eliminated by metabolic pathways (e.g., morphine, midazolam) or by renal excretion (e.g., lamivudine, vancomycin). Moreover, while some drugs have very low adult clearance values (e.g., 0.04 L/h for sulfadoxine and 1.44 L/h for pyrimethamine), drugs such as morphine and propofol have adult *CL* values >100 L/h.

Table III summarizes all fitted parameters. Compared with simple allometry, biphasic allometry fits better, with universally lower *AIC* values (Table III). The allometric coefficients (*A* and *B*) are highly variable among drugs, because the absolute *CL* values span >3 orders of magnitude. However, the allometric exponents have a narrow distribution: the first exponent (α) ranges from 1.51 to 3.67 (mean = 2.36; *CV* = 26%), whereas the second exponent (β) is in the range of 0.40 to 0.67 (mean = 0.55, *CV* = 14%). The mean transitional weight is 10.0 ± 4.9 kg (range = 3.64 to 20.4 kg, *CV* = 49%). The mean transitional slope (*S*^{*}) is 1.46 ± 0.32 (range = 1.0 to 2.0; *CV* = 22%). The results reveal consistent biphasic bodyweight scaling with superlinear-to-sublinear phase transition. Moreover, although the drugs are highly variable in terms of elimination pathways and the magnitude of *CL* value, the characteristic slope of the second phase (i.e., β) is nearly homogenous among different drugs with a *CV* of 14%.

Since the bodyweight at the phase transition has a wider distribution, the 17 drugs were further divided into three groups (Figs. 5, 6 and 7). The bodyweight at the phase transition is around 15 kg for the group I drugs, 10 kg for the group II drugs, and < 5 kg for the group III drugs. The grouping enables visualization and comparison of all 17 drugs with reasonable clarity in three figures. Moreover, it

highlights the similarity and differences of various drugs in the maturation rate.

Finally, to demonstrate the versatility of the biphasic model, the drug clearance values from individual pediatric subjects were retrieved from two studies of cefetamet (48, 49). Figure 8 shows that the biphasic model fits all the datapoints well, except for one point (which is from a subject that had multiple postoperative complications (49)). The fitting results are described in the figure legend. While *A* and *B* values are drug-specific, the α exponent (2.9) falls within the range of the values found for other drugs (Table III). Moreover, the beta exponent (0.47) and the transitional bodyweight (11 kg) are about the mean values estimated for the datasets of 17 drugs.

Unifying All the Datasets

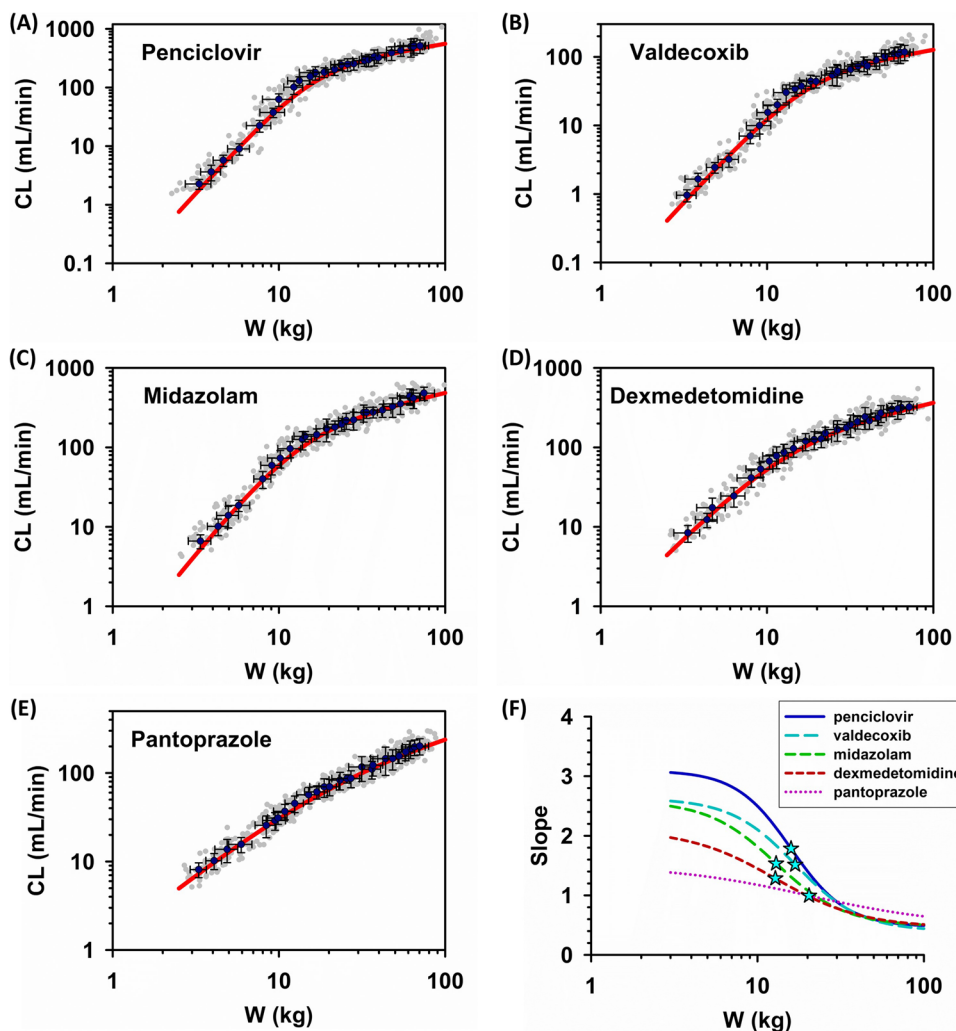
In this study, a total of 25 datasets were included for analysis. These data cover 3 types of human parameters (*BMR*, *GFR*, and drug *CL*), where the absolute values span >3 orders of magnitude. Nevertheless, some common features repeatedly appear throughout this study. To further highlight the similarities and differences among different datasets, a dimensionless analysis was performed, according to the definition of *X* and *Y* and the derived equations (Equations 13,

Table III Fitted and Estimated Parameters for Drug *CL* Datasets

Drug	<i>A</i>	α	<i>B</i>	β	\tilde{w}	<i>S</i> [*]	<i>AIC</i> (<i>BA</i> , <i>SA</i>)
Acetaminophen	0.980	2.05	39.7	0.50	10.8	1.28	(4813, 5317)
Acyclovir	0.042	3.67	21.8	0.63	7.88	2.15	(4909, 5330)
Busulfan	1.170	1.80	24.4	0.51	10.7	1.16	(4269, 4859)
Dexmedetomidine	0.680	2.11	45.8	0.46	12.8	1.29	(4746, 5281)
Lamivudine	0.580	2.26	30.8	0.55	10.2	1.41	(4688, 5242)
Levetiracetam	0.256	1.91	6.05	0.57	10.5	1.24	(2991, 3530)
Levobupivacaine	8.318	1.71	49.6	0.59	4.93	1.15	(5511, 5970)
Midazolam	0.238	2.59	52.9	0.48	12.9	1.54	(5013, 5597)
Morphine	1.732	2.57	125	0.58	8.61	1.58	(6333, 6906)
Pantoprazole	1.383	1.51	31.0	0.48	20.4	1.00	(4079, 4624)
Penciclovir	0.045	3.10	63.6	0.47	15.9	1.79	(5134, 5814)
Propofol	20.13	1.84	129	0.61	4.59	1.23	(6598, 7052)
Pyrimethamine	0.019	3.31	1.23	0.67	4.90	1.99	(2063, 2586)
Ropivacaine	0.084	3.11	40.9	0.53	11.0	1.82	(5070, 5541)
Sulfadoxine	0.005	2.11	0.04	0.67	3.70	1.39	(-1720, -1279)
Valdecoxib	0.037	2.63	20.3	0.40	16.8	1.52	(3574, 4279)
Vancomycin	1.117	1.92	5.87	0.63	3.64	1.28	(3433, 3916)
Mean		2.36		0.55	10.0	1.46	
<i>SD</i>		0.63		0.08	4.9	0.32	
<i>CV</i> (%)		26.4		14.4	49.0	21.9	

The allometric coefficients (*A*, *B*) and bodyweight exponents (α , β) are the best-fitted model parameters (according to Equation 4); $w = (B/A)^{1/(\alpha-\beta)}$ (Equation 8); $S^* = (\alpha + \beta)/2$ (Equation 9); Akaike's information criterion (*AIC*); biphasic allometry model (*BA*); simple allometry model (*SA*).

Fig. 5. Biphasic bodyweight scaling of *CL* (group I drugs). Group I drugs are the drugs with the largest transitional bodyweight (around 15 kg). **A–E** The log *CL* vs. log *W* plots (symbol) and the best-fit lines of the biphasic model. *CL* values with random errors (*CV* = 20%) were generated according to the sigmoidal maturation model (Equations 1–3). Each dataset was fitted to the biphasic model. **F** The slope plots (lines) and the transitional bodyweights (stars) for group I drugs



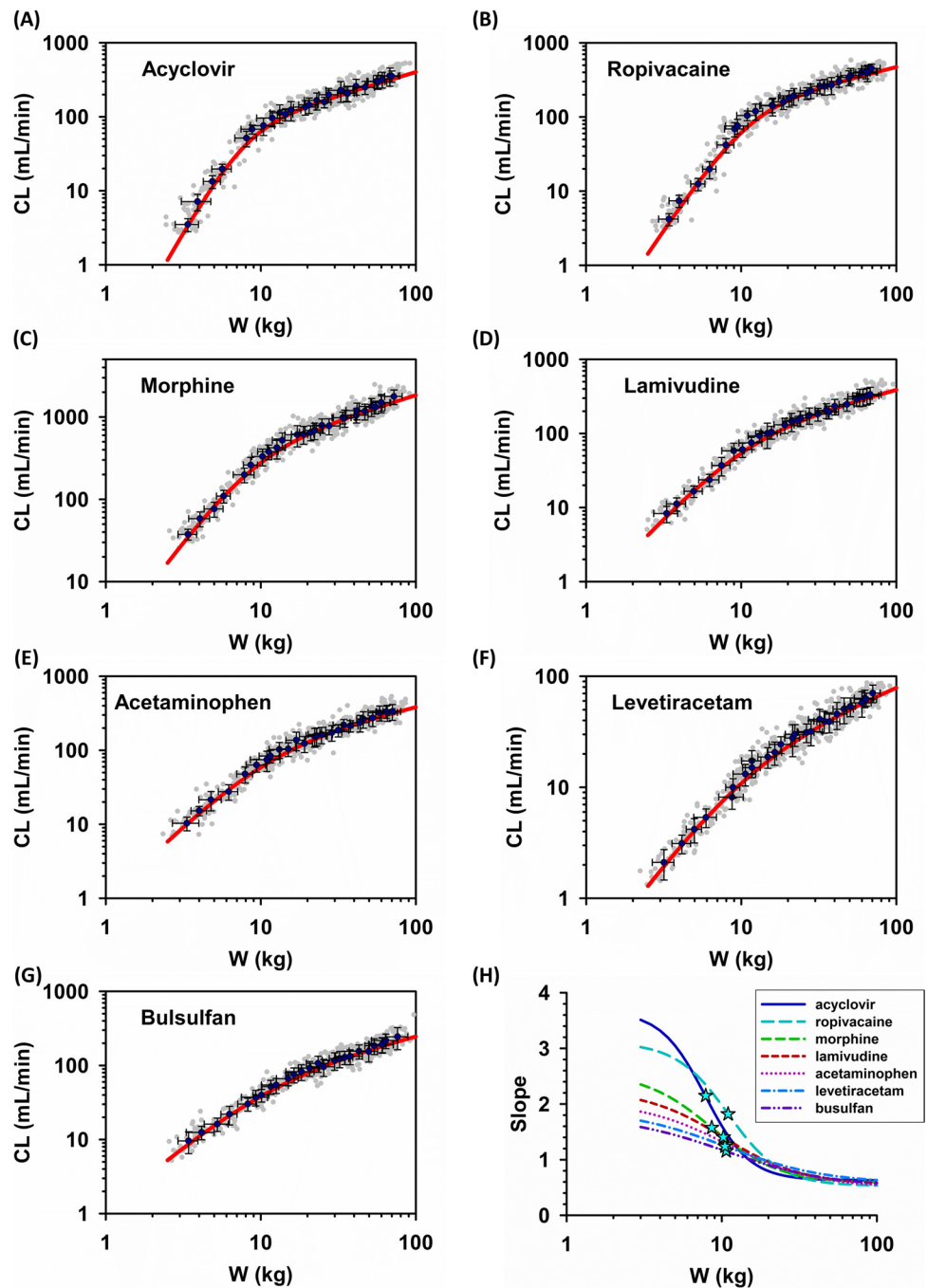
17, and 18). The two new variables (*X*, *Y*) are fractions or multiples of the two characteristic values (\tilde{w} and \tilde{p}). With the dimensionless equation (e.g., Equation 13 or Equation 16), all of the 25 datasets can be compared in one figure (Fig. 9A). This composite plot clearly divides the biphasic curves into two segments at the reference point of (*X*, *Y*) = (1, 1), which is considered as a phase transition (turnaround) point. The first segment is within the region where both *X* and *Y* are below the unity, whereas the second segment locates at (*X*, *Y*) above unity. All the data in the first phase show steeper slopes than those in the second phase (i.e., $\alpha > \beta$). Moreover, the first phase is more variable among different data than the second phase. This is consistent with the magnitude of variability reported in Table III for the drug *CL* (*CV* for α = 26.4%; for β = 14.4%).

Figure 9B further captures the essence of such disparity; while the asymptotic slope in the first phase is distributed from 1.5 to 3.5, the asymptotic slope in the second phase has a narrow distribution (ca. 0.4 to 0.7). A consistent

observation is that all the data seemed to merge at $X > 2$ (i.e., *W* is 2 times that of the transitional bodyweight), suggesting that the maturation and growth patterns of various human parameters are similar when the growing body is passing the critical point of transition.

Figure 9C offers further insights into the deceleration process of human development after birth. By definition, deceleration is the change of the slope of the maturation curve. The negative value suggests that, although the human function is growing, the speed of functional maturation is continuously declining, i.e., deceleration. Figure 9C shows many characteristics of the deceleration process. First, it is an inverse, symmetrical bell-shaped curve with maximal deceleration occurring at the critical turnaround point (1, 1) and, second, slow deceleration in the early life when the body size is small and when the adulthood is approaching. Third, fast deceleration starts almost universally at $X = 0.3$ to 0.4, reaching the maximal deceleration at $X = 1$. This characterizes the maturation pattern of the first phase. After passing the maximal deceleration point, the maturation enters

Fig. 6. Biphasic bodyweight scaling of CL (group II drugs). Group II drugs are the drugs with intermediate transitional bodyweight (around 10 kg). **A–E** The log CL vs. log W plots (symbol) and the best-fit lines of the biphasic model. **F** The slope plots (lines) and the transitional bodyweights (stars) for group II drugs



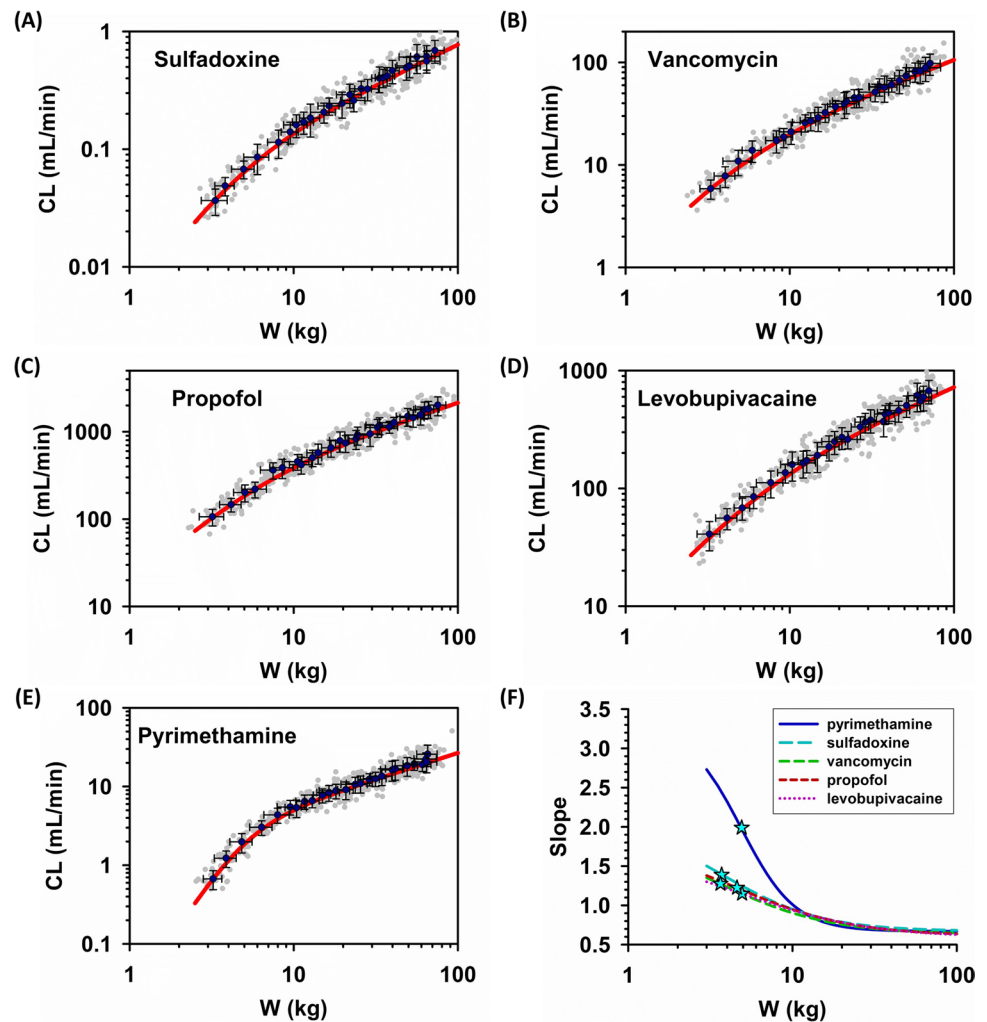
the second phase and, again, approaches zero deceleration at the adulthood (completing the maturation process).

DISCUSSION

The current study proposes a general weight-only equation to model various ontogeny datasets of human parameters. The datasets are diverse, spanning multiple human parameters and covering extensive age groups from birth to adulthood.

The data were either directly retrieved from historical datasets (including mean and individual values) or simulated from independent models with published values for specific model parameters. A statistical random sampling approach was used to add random errors to the simulated data. The results demonstrate that a biphasic, mixed-power-law equation with two limiting allometric functions adequately quantifies the developmental phase transition profiles of BMR , GFR , and drug CL . The biphasic model and the additional

Fig. 7. Biphasic bodyweight scaling of CL (group III drugs). Group III drugs are the drugs with the lowest transitional bodyweight (< 5 kg). **A–E** The log CL vs. log W plots (symbol) and the best-fit lines of the biphasic model. **F** The slope plots (lines) and the transitional bodyweights (stars) for group III drugs



dimensionless analysis offer quantitative insights into the maturation and growth of human body functions.

The long-held belief that body functions develop at distinct pace in different stages of human development is well supported by extensive empirical evidence (1, 5, 52–54). For example, a study dated back to 1949 had shown that renal function matures with the most rapid rate in the first 6 months, followed by slower rates to reach adult values around the second year of life (52). Numerous empirical models have been proposed to scale the maturation and growth processes of body functions (6, 7, 24). These quantitative equations have been frequently developed for practical considerations, e.g., estimating children's values (6, 14, 39). The equations are usually data-specific and age-categorized. Most equations contain bodyweight as an input variable; meanwhile, age was often included as an additional variable (6–8, 24, 36). The equations are either separate, discontinuous equations with cut-points at certain age thresholds (23, 40), or continuous nonlinear equations containing age and bodyweight terms (7, 8, 15, 24). The dependence of bodyweight on age (55–57) is often required to assume a fixed

weight exponent value (i.e., 0.75) in order to estimate the age-associated parameters (e.g., maturation half-life and Hill coefficient) (15, 24, 58). Accordingly, this present study provides a different perspective where bodyweight alone in a continuous 4-parameter power-law equation is sufficient to quantitatively describe the maturation process.

A previous study has shown that the brain's metabolic requirement starts to accelerate after the first 6-month of life and reaches a lifetime peak at about 5 years of age (1). During this particular period, the increasing demand of energy in human brain development was compensated by slow rate of body growth (1). This present study reveals that the rate switching of BMR , GFR , and CL occurs at bodyweights of around 5–20 kg, which is about the bodyweight range for children of 0.5–9 years of age. Moreover, the transitional bodyweights for different datasets center around 10 kg, which is about the weight of children at 1 year of age.

The biphasic profiles are universally reproduced in different datasets. Since other important metabolic organs, such as the liver and the kidneys, may develop similar age-related dynamics in energy demands, the biphasic profiles

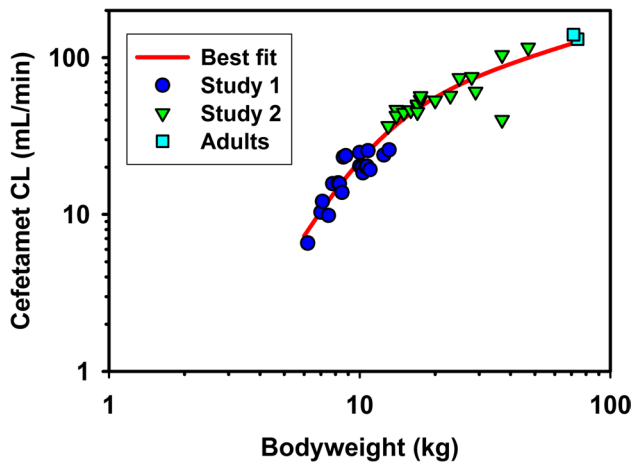


Fig. 8. Biphasic bodyweight scaling of individual pediatric *CL* data obtained from different pharmacokinetic studies. The individual *CL* values of cefetamet were retrieved from study 1 (20 infants, 0.19 to 1.44 years)(48) and study 2 (18 children, 3 to 12 years)(49). The adult data were from ref. (50, 51). One subject in the second study was reported to have multiple postoperative complications (coincidentally, the one that has a *CL* value far below the fitted line). The pooled data were fitted with the biphasic allometry and the simple allometry model. The *AIC* values are 269 (biphasic) vs. 313 (simple allometry). The fitted parameter values for the basic model are $A = 0.049$, $\alpha = 2.90$, $B = 16.6$, and $\beta = 0.47$. The estimated transition bodyweight is 11.0 kg

may be associated with the trade-off between maturation (functional development) and growth (body size development). In the first developmental phase, high blood perfusion organs (e.g., brain, liver, kidney) take up more metabolic substrate (e.g., glucose) to allow fast development of organ functions (fast maturation), which results in less energy available for the building of body mass (slow growth). Therefore, this phase is characterized by high energy needs for the maturation of vital organs, leading to the superlinear bodyweight scaling relations (exponent > 1). At birth, the major drug eliminating organs continue to mature and grow. The sizes of these organs grow at different paces, with fractional organ size (i.e., weight per kg bodyweight) reaching the maximum at around 1 to 2 years of age (59). The organ blood flow also increases with age and bodyweight at different rates (29, 60–62). Moreover, the enzyme activities (per kg bodyweight) of most drug metabolizing enzymes (e.g., *CYP 3A4*) also undergo fast maturation and reach the adult levels at around 1–2 years of age, although some enzyme may mature faster or slower (60, 61). The above-mentioned characteristic ages of maturation correspond to average bodyweight of 9 to 13 kg (43); coincidentally, the mean transition bodyweight (10.0 kg) observed for the drug *CL* datasets (Table III) falls within the range. Compared to the later phase, the first phase has greater variability in the estimated asymptotic

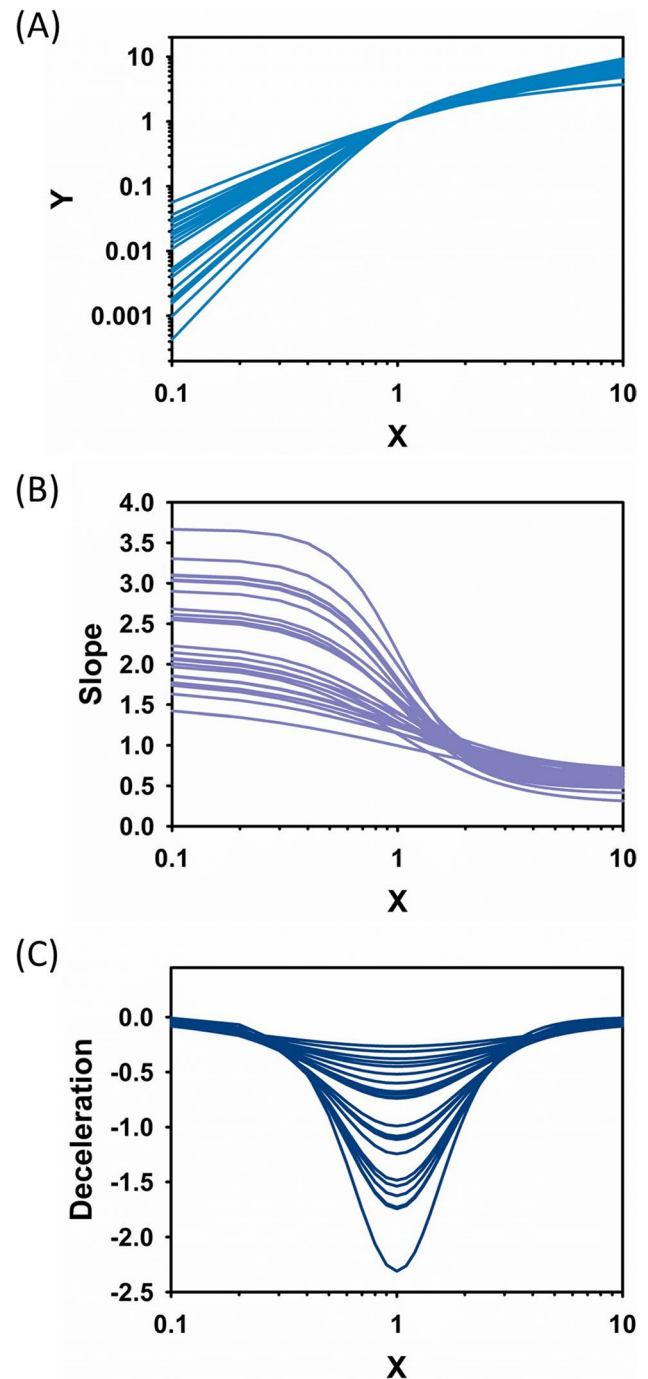


Fig. 9. Unifying 25 datasets using dimensionless analysis. **A** The log–log plot for the dimensionless variables. **B** The slope plots. **C** The deceleration plots. The definitions of the dimensionless variables, X (fractional W) and Y (fractional P), and of the slope and deceleration are described in Section - Dimensionless Analysis. For each individual dataset, the fitted parameters of the biphasic model were used to simulate the dimensionless data, using Equations 13, 17, and 18. A total of 25 datasets (covering *BMR*, *GFR*, and drug *CL*) were compared in one plot

(α) exponent ($CV = 26\%$). The CV for the transitional bodyweight is even larger (49%); however, the variability

levels are still surprisingly low, if one considers that the drugs differ widely both in the exact *CL* values and elimination mechanisms. The results suggest commonality and variability in ontogeny. While both features warrant further empirical and theoretical investigations, the variability may be attributed to variation in the maturation speed of various factors (hepatic, renal, biliary, and blood) that contribute to overall drug elimination in the maturing and growing body (59–68).

As the body size development enters into another phase, the energy supply relative to the maturing vital organs might need to be bounded or be re-shuffled to other organs, e.g., muscle. This may contribute to continuous decrease of metabolism and many other organ functions along the maturation process (69). In the present paper, equations are derived to quantify this deceleration process, which reaches the maximal deceleration at the transitional bodyweight and proceeds to the second phase. Notably, the deceleration profile is symmetrical at the transitional point (Fig. 9C). Since in the second phase, growth of body size dominates functional maturation, the phase is less variable, characterized by tightly disturbed asymptotic exponent with low *CV* (14%, Table III) and by highly superimposed slope profiles after passing the transitional point (Fig. 9B). Taken together, energy re-allocation between high and low energy-demanding organs may attribute to biphasic maturation and growth of organ functions. This view is consistent with the general model of West *et al.* (55) which suggests that the growth of body size is limited by the capacity of resource allocation networks.

As illustrated in the Appendix (Fig. 10 in the Appendix), the curvature of the biphasic profile is set by the two allometric functions. Each of the two extreme states is represented by a single allometric function of bodyweight raised to a constant power (α or β). The magnitude of the two exponents shapes the entire curve: for example, higher α together with lower β produces greater curvature and more obvious phase transitions, as indicated in the modeling of the *CL* values for 17 drugs (Table III and Figs. 5, 6 and 7). Moreover, the biphasic model shows that the slope of the scaling curve continuously changes during the developmental period, which agrees with previous observations (16, 28, 30).

The essence of the phase switching with deceleration is further captured by the dimensionless analysis. According to Equation 13 (or Equation 16), all unitless data will converge at $(X, Y) = (1, 1)$, which is also the transition point of the biphasic curve. The dimensionless equations indicate that metabolic and physiological functions scale with bodyweight superlinearly at $X < 1$ (i.e., bodyweight < transitional weight) and sublinearly at $X > 1$ (i.e., bodyweight > transitional weight). The dimensionless analysis can be further elaborated as follows. Mathematically, Equation 17 can be expressed as the linear combination of two fractional terms:

$$\text{slope} = \alpha \cdot f_{\beta} + \beta \cdot f_{\alpha} \quad (19)$$

where

$$0 < f_{\alpha} = \frac{X^{\alpha}}{X^{\alpha} + X^{\beta}} < 1 \quad (20)$$

$$0 < f_{\beta} = \frac{X^{\beta}}{X^{\alpha} + X^{\beta}} < 1 \quad (21)$$

and the deceleration equation (Equation 17) can be simplified as

$$\text{deceleration} = -(\alpha - \beta)^2 f_{\alpha} \cdot f_{\beta} \quad (22)$$

In biological terms, the two fractions represent the relative contribution of the two maturation/growth phases (i.e., α and β phases) from birth to adulthood. Phase transition occurs at the characteristic bodyweight where the two phases have equal contribution (i.e., $f = 1/2$). Thus, at the phase transition point, the slope is the average of the two characteristic exponents, i.e., $(\alpha + \beta)/2$, and deceleration reaches the maximal value $-0.25(\alpha - \beta)^2$. In this study, the β exponent is around 0.5 with small variation across all 25 datasets. In contrast, the α exponent has larger variation (Table III and Fig. 9B). Thus, larger difference in the two exponents results in sharper transition and greater peak deceleration (Fig. 9C).

Bodyweight has been proposed and evaluated as the covariate in predicting pediatric *CL* values. It is known that a fixed exponent is insufficient to describe the change of *CL* with respect to bodyweight increases across the human lifespan. Given that the bodyweight exponent value is usually higher in younger (e.g., neonates and infants) than in older age groups, the bodyweight exponent has been treated as a continuous function that features continuous decline of exponent during growth—the so-called bodyweight-dependent exponent (BDE) models. Table IV compares the BDE models with the biphasic model. The first BDE model (BDE I) assumes that the decline of exponent follows a 4-parameter sigmoidal bodyweight function, with clearly defined maximal and minimal exponents. The model has been applied in the population pharmacokinetic analysis of two drugs (propofol and morphine), covering subjects with bodyweight ranging from 0.56 to 122.7 kg (2 studies)(16, 70). As demonstrated in these 2 studies, the inclusion of 4 parameters in the exponent function would have an advantage of modeling data including preterm neonates with extreme low bodyweight. However, it would be more challenging to estimate all the parameters with confidence, especially when the neonate data are not sufficient.

The second BDE model (BDE II) also includes a bodyweight-dependent exponent function, which itself is also a power-law function, with 2 parameters that characterize the weight-dependent decline of exponent. The model has been

Table IV Comparison of Continuous Bodyweight-Dependent Exponent (BDE) Models with the Biphasic Model

Models	Equations	Model features	Demonstrated cases and remarks
BDE I	$CL = a \cdot \left(\frac{W}{W_{ref}} \right)^{k(W)}$ <p>a, reference CL at $W = W_{ref}$; $k(W)$, W-dependent exponent function</p> $k(W) = k_0 - \frac{k_{max} \times W^n}{k_0 + W^n}$	<ul style="list-style-type: none"> Assigning a 4-parameter sigmoidal function, $k(W)$, to quantify the W-dependent decline of exponent Exponent declining from k_0 (the exponent at “$W = 0$ kg”) to $k_0 - k_{max}$ (maximal decline); $k_{50} = W$ at 50% of the maximal decline; steepness shaped by the Hill coefficient (n) Requiring fixation of some parameters to estimate the other parameters 	Population pharmacokinetic (PPK) studies of propofol (16) and morphine (70); covering preterm and term neonates with low bodyweights (i.e., 0.6 to 3 kg); $W_{ref} = 70$ kg
BDE II	$CL = a \cdot \left(\frac{W}{W_{ref}} \right)^{k(W)}$ <p>a, reference CL at $W = W_{ref}$; $k(W)$, W-dependent exponent function. $k(W) = b \cdot W^{-c}$</p>	<ul style="list-style-type: none"> Assigning a 2-parameter power-law function, $k(W)$, to quantify the W-dependent decline of exponent Exponent = b at $W = 1$ kg, declining with increasing W at a constant speed, c, on the log scales (i.e., $d \ln k/d \ln W = -c$) 	PPK studies of busulfan (71), $W_{ref} = 15.3$ kg; model comparison in the prediction of pediatric CL for several drugs (3, 33) and GFR (6), $W_{ref} = 70$ kg; scaling CL of factor VIII and factor IX from infants to adults (72), $W_{ref} = 70$ kg
Biphasic model	$\frac{1}{P} = \frac{1}{A \cdot W^\alpha} + \frac{1}{B \cdot W^\beta}$ <p>$P = BMR, GFR$, or CL; A, B, allometric coefficients; α, β, allometric exponents</p>	<ul style="list-style-type: none"> Two-phase growth/maturation characterized by two asymptotic allometric functions Characteristic transitional bodyweight derived and defined A slope function featuring the phase-dependent, continuous decline of growth/maturation speed The continuous deceleration captured by a symmetric function showing the peak deceleration Dimensionless analysis revealing simplicity and generality 	Modeling of 3 human parameters (BMR, GFR , and CL) using historical and simulated datasets; phase transition, and deceleration concept clearly illustrated by the dimensionless analysis (this study)

applied in three contexts: the population pharmacokinetic analysis of busulfan (71), predicting drug CL in children (3, 33), and scaling CL of clotting factor VIII and IX (72). Specifically, the model has been compared to other methods, including simple allometry with single fixed exponent (0.75 or data-specific), age-dependent exponent (ADE) model, segmented model, and/or maturation model (3, 33). Overall, the predictive power of the models varied with drugs or with age groups (33); however, the BDE model seemed to provide better prediction of drug CL for theophylline (3) and the clotting factors (72).

Compared with the BDE models, the biphasic model proposed in this study represents a completely different concept and methodology (Table IV). The model combines simple allometry in a form of inverse function. The two allometric exponent terms (α and β) shape the curvature of ontogeny bodyweight profiles with two distinct, definable phases. Besides, the allometric coefficient terms (A and B) determine the absolute value of human parameters (i.e., BMR , GFR , and CL of different drugs). Moreover, the model offers meaningful insights into the ontogeny dynamics of human functions. The simplicity and generality of the biphasic model are revealed in several derived terms: phase transition bodyweight, slope (rate of ontogeny), and deceleration (reduction of ontogeny rate).

Besides BDE, the age-dependent exponent (ADE) model has been previously applied to predict clearance in children. The ADE model assigns different exponent values for different age groups (3, 33, 73): 1.2 (0–3 months), 1.0 (>3 months – 2 years), 0.9 (>2–5 years), and 0.75 (>5 years). In terms of predictive performance, the ADE model appears to be comparable with BDE II (3, 33) and PBPK models (73). Since the exponent values are pre-determined, the ADE model may be useful in helping the design of first-in-child pharmacokinetic studies during new drug development (3, 33). The issue with the ADE model, however, is the designation of the same fixed exponents within the same age group for different drugs. In this study, the proposed biphasic model shows that the slope of the ontogeny curve changes continuously with bodyweight (e.g., Figs. 5F, 6H, 7F), and the slope of the early-life phase is much higher than the largest designated exponent (i.e., 1.2) in the ADE model. From this perspective, the biphasic model may help refine the ADE model by estimating the age group- and compound (or dataset)-specific exponent values using Equation 7.

Some caveats and future perspectives are noted here. The aim of this study is *not* to predict the unknown values from the proposed model. Instead, the study is the first attempt aiming to understand the ontogeny process of human metabolism and physiological functions by proposing a general, harmonizing model. Future studies may be directed

towards building and validating the proposed model for practical applications, such as prediction of renal functions, of pediatric doses and of metabolic demands. Such studies would have broad implications in new drug development, clinical drug therapy (74–77), and clinical nutrition (78–80). However, it should be noted that all prediction models may be suitable for predicting mean population values but not for individual prediction, because the observed value for an individual child is erratic and uncertain (33). During pediatric new drug development, BDE and other allometric models may lack practical application due to limited availability of data (33). The biphasic model may have the same issue. However, the current study demonstrates that α

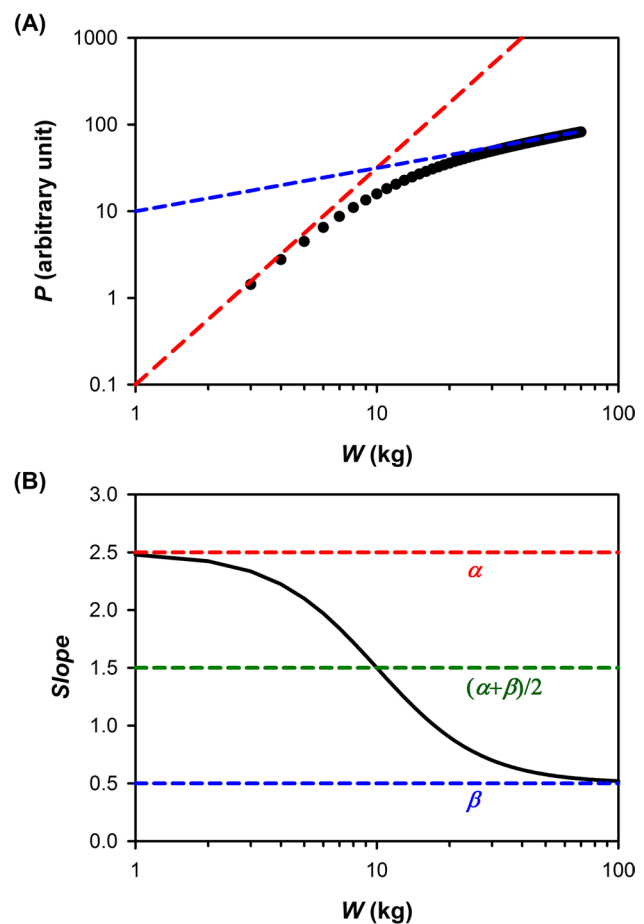


Fig. 10 Characteristics of the mixed-power function. **A** Simulated data of physiological quantity (P) vs. bodyweight (W). The lines represent the two asymptotic power-law functions with respective y -intercepts (i.e., 0.1 and 10, at $W = 1$ kg) and an interception point which defines the critical point of phase transition (at $W = 10$ kg). **B** Slope as a function of bodyweight. The plot highlights the two allometric exponents (α and β) and the corresponding mean value at the point of phase transition

and β are narrowly distributed with $CV\%$ of 26% and 14%, respectively, although the drugs differ widely in their absolute CL values (> 3 orders of magnitude) and in elimination mechanisms (metabolism-dominated vs. renal excretion-dominated). Future studies may lead to further classification of drugs according to the parameter values and drug properties, e.g., elimination mechanisms. For example, for a new investigational drug that is mainly renally excreted, the proposed dimensionless model (Equation 13 or 16) may be used for predicting pediatric CL of the drug, using the parameter values obtained from the GFR dataset. The proposed dimensionless form asks only for two parameters, i.e., α and β . For application, it remains only to specify the phase transition bodyweight, which will then determine the CL value at this characteristic weight. The mean phase transition weight (10 kg) may be used; alternatively, specific weight may be used if the drug can be classified into specific ontogeny group. Moreover, the same reasoning and approach may be applied in population pharmacokinetic analysis and PBPK modeling. The dimensionless equation will be applied to transformed, unitless CL and weight values. Finally, this paper may inspire future attempts in finding a theoretical framework and derivation of the equation based on first principles.

CONCLUSION

In this paper, a general equation is proposed to model the maturation of BMR , GFR , and drug CL . The equation (Equation 4) is expressed in reciprocal terms of mixed allometric functions where bodyweight is the only independent variable. All the bodyweight-based profiles are biphasic on log–log coordinates. The biphasic curvature is determined by two asymptotic allometric functions, representing the maturation and growth functions, respectively. The first phase (below the critical bodyweight) is universally characterized by much steeper slopes with an asymptotic exponent > 1 (superlinear scaling). The second phase (above the critical bodyweight), however, exhibits much shallower slopes with an asymptotic exponent < 1 (sublinear scaling). The proposed equation can be further expressed in a unitless form, where the relationship between the fractional physiological/metabolic quantity (Y) and the fractional bodyweight (X) can be described by a general equation with two allometric exponents, α and β . The unified equation quantitatively characterizes the curvature of the biphasic maturation and growth profiles for diverse datasets, by two characteristic parameters (α and β). In conclusion, the proposed mixed-allometry model enables a quantitative understanding of human development from birth to adulthood.

APPENDIX

Characteristics of the Biphasic Model

This study proposes a mixed-power function (the biphasic allometry model) (Equation 4) to scale human BMR , GFR , and drug CL from adults to neonates. In fact, this study was inspired by allometric scaling of whole-plant respiration from small seedlings to giant trees (12). Equation 4 states that the reciprocal of a physiological or metabolic parameter (P) is equal to the sum of reciprocals of each of two individual power-law bodyweight functions (i.e., allometric functions). To understand the key features of the model, a simulation was conducted to characterize the mixed-power function. The following hypothetical parameters were used: $A = 0.1$, $B = 10$, $\alpha = 2.5$, and $\beta = 0.5$. By plugging the parameter values into Equation 4, a set of hypothetical (P , W) data was generated for a simulated bodyweight range of 3–70 kg (at a 1-kg interval). Figure 10A shows the simulated data and two asymptotic lines on log–log coordinates. Let P_1 and P_2 be the first and second asymptotic functions, respectively, and then the asymptotic bodyweight functions are

$$P_1 = AW^\alpha \quad (23)$$

$$P_2 = BW^\beta \quad (24)$$

and Equation 4 can be expressed as

$$\frac{1}{P} = \frac{1}{P_1} + \frac{1}{P_2} \quad (25)$$

when $P_1 \ll P_2$, $P \approx P_1$, which is the first asymptote near the low bodyweight region of $W \ll (B/A)^{1/(\alpha-\beta)}$ (by solving the inequality relationship). In contrast, when $P_1 \gg P_2$, $P \approx P_2$, the second asymptote occurs at $W \gg (B/A)^{1/(\alpha-\beta)}$. Thus, the characteristic bodyweight (\tilde{w}) is revealed as

$$\tilde{w} = (B/A)^{1/(\alpha-\beta)} \quad (26)$$

Mathematically, \tilde{w} is exactly the bodyweight at which the two asymptotic lines intersect ($P_1 = P_2$ and $A\tilde{w}^\alpha = B\tilde{w}^\beta$). Biologically, it is considered here as the critical bodyweight at which the body undergoes transition from maturation phase to growth phase (i.e., the phase transition bodyweight). By taking the derivative of Equation 4, the following expression for the slope (S) of the biphasic curve is obtained:

$$S = \frac{d \log P}{d \log W} = \beta \left(\frac{P_1}{P_1 + P_2} \right) + \alpha \left(\frac{P_2}{P_1 + P_2} \right) \quad (27)$$

Therefore, according to Equation 27, the slope of the biphasic model can be estimated at any given bodyweight. Figure 10B shows that the slope decreases with increasing bodyweight. The slope curve is indeed flanked by two asymptotic lines: slope $\approx \alpha$, at the low body weight region where $W \ll \tilde{w}$ or when $P_1 \ll P_2$; whereas slope $\approx \beta$, at $W \gg \tilde{w}$ or when $P_1 \gg P_2$. Note that the characteristic slope (S^*) at the phase transition bodyweight is exactly the mean of the two asymptotic exponents, since at $W = w$, $P_1 = P_2$, Equation 27 is reduced to

$$S^* = (\alpha + \beta)/2 \quad (28)$$

In sum, Fig. 10 captures the essence of the proposed mixed-allometry model by revealing all the parameter values used for the simulation: two asymptotic exponents of 2.5 and 0.5 (exactly α and β), two asymptotic allometric coefficients ($A = 0.1$, $B = 10$), and a critical bodyweight of 10 kg (i.e., $\tilde{w} = (B/A)^{1/(\alpha-\beta)} = (10/0.1)^{1/2}$) where the slope of the biphasic curve at this critical point is exactly the mean of the two exponents (i.e., 1.5).

Author Contribution Teh-Min Hu is the sole author who contributes to the conception of the work and acquisition, analysis, and interpretation of data and performs modeling and simulation, derivations of equations, and writing, revising, and submitting the manuscript.

Funding The author is supported by the Ministry of Science and Technology (MOST) and Higher Education Sprout Project — Ministry of Education (MOE), Taiwan.

Declarations

Conflict of Interest The author declares no competing interests.

References

- Kuzawa CW, Chugani HT, Grossman LI, Lipovich L, Muzik O, Hof PR, Wildman DE, Sherwood CC, Leonard WR, Lange N. Metabolic costs and evolutionary implications of human brain development. *Proc Natl Acad Sci*. 2014;111(36):13010–5.
- Pontzer H, Brown MH, Raichlen DA, Dunsworth H, Hare B, Walker K, Luke A, Dugas LR, Durazo-Arvizu R, Schoeller D. Metabolic acceleration and the evolution of human brain size and life history. *Nature*. 2016;533(7603):390–2.
- Tegenge MA, Mahmood I. Age- and bodyweight-dependent allometric exponent model for scaling clearance and maintenance dose of theophylline from neonates to adults. *Ther Drug Monit*. 2018;40(5):635–41.
- Bowes HM, Burdon CA, Taylor NA. The scaling of human basal and resting metabolic rates. *Eur J Appl Physiol*. 2021;121(1):193–208.
- O’flaherty EJ. Physiologic changes during growth and development. *Environ Health Perspect*. 1994;102(suppl 11):103–6.
- Mahmood I, Staschen C-M. Prediction of human glomerular filtration rate from preterm neonates to adults: evaluation of predictive performance of several empirical models. *AAPS J*. 2016;18(2):445–54.
- Hayton WL. Maturation and growth of renal function: dosing renally cleared drugs in children. *AAPS PharmSci*. 2000;2(1):22–8.
- Calvier E, Krekels E, Johnson T, Rostami-Hodjegan A, Tibboel D, Knibbe CA. Scaling drug clearance from adults to the young children for drugs undergoing hepatic metabolism: a simulation study to search for the simplest scaling method. *AAPS J*. 2019;21(3):1–11.
- Klingenberg CP. Heterochrony and allometry: the analysis of evolutionary change in ontogeny. *Biol Rev*. 1998;73(1):79–123.
- Glazier DS. Beyond the ‘3/4-power law’: variation in the intra- and interspecific scaling of metabolic rate in animals. *Biol Rev*. 2005;80(4):611–62.
- Glazier DS. Is metabolic rate a universal ‘pacemaker’ for biological processes? *Biol Rev*. 2015;90(2):377–407.
- Mori S, Yamaji K, Ishida A, Prokushkin SG, Masyagina OV, Hagihara A, Hoque AR, Suwa R, Osawa A, Nishizono T. Mixed-power scaling of whole-plant respiration from seedlings to giant trees. *Proc Natl Acad Sci*. 2010;107(4):1447–51.
- DeLong JP, Okie JG, Moses ME, Sibly RM, Brown JH. Shifts in metabolic scaling, production, and efficiency across major evolutionary transitions of life. *Proc Natl Acad Sci*. 2010;107(29):12941–5.
- Germovsek E, Barker CI, Sharland M, Standing JF. Scaling clearance in paediatric pharmacokinetics: all models are wrong, which are useful? *Br J Clin Pharmacol*. 2017;83(4):777–90.
- Holford N, Heo Y-A, Anderson B. A pharmacokinetic standard for babies and adults. *J Pharm Sci*. 2013;102(9):2941–52.
- Wang C, Peeters MY, Allegaert K, van Oud-Alblas HJB, Krekels EH, Tibboel D, Danhof M, Knibbe CA. A bodyweight-dependent allometric exponent for scaling clearance across the human lifespan. *Pharm Res*. 2012;29(6):1570–81.
- Mahmood I. Prediction of drug clearance in children from adults: a comparison of several allometric methods. *Br J Clin Pharmacol*. 2006;61(5):545–57.
- Henry C. Basal metabolic rate studies in humans: measurement and development of new equations. *Public Health Nutr*. 2005;8(7a):1133–52.
- EFSA Panel on Dietetic Products N & Allergies. Scientific opinion on nutrient requirements and dietary intakes of infants and young children in the European Union. *EFSA J*. 2013;11(10):3408.
- Oussaada SM, van Galen KA, Cooiman MI, Kleinendorst L, Hazebroek EJ, van Haelst MM, Ter Horst KW, Serlie MJ. The pathogenesis of obesity. *Metabolism*. 2019;92:26–36.
- Kliemann N, Murphy N, Viallon V, Freisling H, Tsilidis KK, Rinaldi S, Mancini FR, Fagherazzi G, Boutron-Ruault MC, Boeing H. Predicted basal metabolic rate and cancer risk in the European Prospective Investigation into Cancer and Nutrition. *Int J Cancer*. 2020;147(3):648–61.
- Den Broeder E, Oeseburg B, Lippens R, Van Staveren W, Sengers R, van’t Hof M, Tolboom J. Basal metabolic rate in children with a solid tumour. *Eur J Clin Nutr*. 2001;55(8):673–81.
- WHO (2004) *Human energy requirements: report of a joint FAO/WHO/UNU expert consultation: Rome, 17-24 October 2001* (Food & Agriculture Org.).
- Rhodin MM, Anderson BJ, Peters AM, Coulthard MG, Wilkins B, Cole M, Chatelut E, Grubb A, Veal GJ, Keir MJ. Human renal function maturation: a quantitative description using weight and postmenstrual age. *Pediatr Nephrol*. 2009;24(1):67–76.
- Liu T, Ghafoori P, Gobburu JV. Allometry is a reasonable choice in pediatric drug development. *J Clin Pharmacol*. 2017;57(4):469–75.
- Strougo A, Eissing T, Yassen A, Willmann S, Danhof M, Freijer J. First dose in children: physiological insights into pharmacokinetic

- scaling approaches and their implications in paediatric drug development. *J Pharmacokinet Pharmacodyn.* 2012;39(2):195–203.
27. Brussee JM, Krekels EH, Calvier EA, Palić S, Rostami-Hodjegan A, Danhof M, Barrett JS, de Wildt SN, Knibbe CA. A pediatric covariate function for CYP3A-mediated midazolam clearance can scale clearance of selected CYP3A substrates in children. *AAPS J.* 2019;21(5):1–11.
 28. Wang C, Allegaert K, Peeters MY, Tibboel D, Danhof M, Knibbe CA. The allometric exponent for scaling clearance varies with age: a study on seven propofol datasets ranging from preterm neonates to adults. *Br J Clin Pharmacol.* 2014;77(1):149–59.
 29. Björkman S. Prediction of drug disposition in infants and children by means of physiologically based pharmacokinetic (PBPK) modelling: theophylline and midazolam as model drugs. *Br J Clin Pharmacol.* 2005;59(6):691–704.
 30. Calvier EA, Krekels EH, Väitalo PA, Rostami-Hodjegan A, Tibboel D, Danhof M, Knibbe CA. Allometric scaling of clearance in paediatric patients: when does the magic of 0.75 fade? *Clin Pharmacokinet.* 2017;56(3):273–85.
 31. Colin PJ, Allegaert K, Thomson AH, Touw DJ, Dolton M, de Hoog M, Roberts JA, Adane ED, Yamamoto M, Santos-Buelga D. Vancomycin pharmacokinetics throughout life: results from a pooled population analysis and evaluation of current dosing recommendations. *Clin Pharmacokinet.* 2019;58(6):767–80.
 32. Wu Q, Peters SA. A retrospective evaluation of allometry, population pharmacokinetics, and physiologically-based pharmacokinetics for pediatric dosing using clearance as a surrogate. *CPT Pharmacometrics Syst Pharmacol.* 2019;8(4):220–9.
 33. Mahmood I, Staschen C-M, Goteti K. Prediction of drug clearance in children: an evaluation of the predictive performance of several models. *AAPS J.* 2014;16(6):1334–43.
 34. van Groen BD, Pilla Reddy V, Badée J, Olivares-Morales A, Johnson TN, Nicolaï J, Annaert P, Smits A, de Wildt SN, Knibbe CA. Pediatric pharmacokinetics and dose predictions: a report of a satellite meeting to the 10th Juvenile Toxicity Symposium. *Clinical and Translational Science.* 2021;14(1):29–35.
 35. Foissac F, Bouazza N, Valade E, De Sousa MM, Fauchet F, Benaboud S, Hirt D, Tréluyer JM, Urien S. Prediction of drug clearance in children. *J Clin Pharmacol.* 2015;55(7):739–47.
 36. Lonsdale DO, Baker EH, Kipper K, Barker C, Philips B, Rhodes A, Sharland M, Standing JF. Scaling beta-lactam antimicrobial pharmacokinetics from early life to old age. *Br J Clin Pharmacol.* 2019;85(2):316–46.
 37. Anderson BJ, Holford NH. Mechanistic basis of using body size and maturation to predict clearance in humans. *Drug metabolism and pharmacokinetics.* 2009;24(1):25–36.
 38. Krekels EHJ, Calvier EAM, van der Graaf PH, Knibbe CAJ. Children are not small adults, but can we treat them as such? *CPT Pharmacometrics Syst Pharmacol.* 2019;8(1):34–8.
 39. Mansoor N, Ahmad T, Khan RA, Sharib SM, Mahmood I. Prediction of clearance and dose of midazolam in preterm and term neonates: a comparative study between allometric scaling and physiologically based pharmacokinetic modeling. *Am J Ther.* 2019;26(1):e32–7.
 40. Shimamura K, Wajima T, Yano Y. Pharmacokinetic prediction for intravenous β -lactam antibiotics in pediatric patients. *J Pharm Sci.* 2007;96(11):3125–39.
 41. Schofield WN. Predicting basal metabolic rate, new standards and review of previous work. *Hum Nutr Clin Nutr.* 1985;39:5–41.
 42. Anderson BJ, Holford NH. Mechanism-based concepts of size and maturity in pharmacokinetics. *Annu Rev Pharmacol Toxicol.* 2008;48:303–32.
 43. WHO (1985) *Energy and protein requirements: report of a Joint FAO/WHO/UNU Expert Consultation [held in Rome from 5 to 17 October 1981]* (World Health Organization).
 44. Lacey L, Keene O, Pritchard J, Bye A. Common noncompartmental pharmacokinetic variables: are they normally or log-normally distributed? *J Biopharm Stat.* 1997;7(1):171–8.
 45. Gualandi S, Toscani G. Human behavior and lognormal distribution. A kinetic description. *Mathematical Models and Methods in Applied Sciences.* 2019;29(04):717–53.
 46. Daly L, Bourke GJ. Interpretation and uses of medical statistics: (John Wiley & Sons); 2008.
 47. Kirkwood TB (1979) Geometric means and measures of dispersion. *Biometrics:*908–909.
 48. Hayton WL, Kneer J, de Groot R, Stoeckel K. Influence of maturation and growth on cefetamet pivoxil pharmacokinetics: rational dosing for infants. *Antimicrob Agents Chemother.* 1996;40(3):567–74.
 49. Hayton W, Walstad R, Thurmann-Nielsen E, Kufas T, Kneer J, Ambros R, Rugstad H, Monn E, Bodd E, Stoeckel K. Pharmacokinetics of intravenous cefetamet and oral cefetamet pivoxil in children. *Antimicrob Agents Chemother.* 1991;35(4):720–5.
 50. Koup JR, Dubach U, Brandt R, Wyss R, Stoeckel K. Pharmacokinetics of cefetamet (Ro 15-8074) and cefetamet pivoxil (Ro 15-8075) after intravenous and oral doses in humans. *Antimicrob Agents Chemother.* 1988;32(4):573–9.
 51. Kneer J, Tam Y, Blouin R, Frey F, Keller E, Stathakis C, Luginbuehl B, Stoeckel K. Pharmacokinetics of intravenous cefetamet and oral cefetamet pivoxil in patients with renal insufficiency. *Antimicrob Agents Chemother.* 1989;33(11):1952–7.
 52. Rubin MI, Bruck E, Rapoport M, Snively M, McKay H, Baumler A. Maturation of renal function in childhood: clearance studies. *J Clin Investig.* 1949;28(5):1144–62.
 53. Bogin B. Patterns of human growth: (Cambridge University Press); 2020.
 54. Holliday M (1971) Metabolic rate and organ size during growth from infancy to maturity and during late gestation and early infancy. *Pediatrics* 47(1):Suppl 2: 169+–Suppl 162: 169+.
 55. West GB, Brown JH, Enquist BJ. A general model for ontogenetic growth. *Nature.* 2001;413(6856):628–31.
 56. Sumpter AL, Holford NH. Predicting weight using post-menstrual age–neonates to adults. *Pediatr Anesth.* 2011;21(3):309–15.
 57. Meibohm B, Läer S, Panetta JC, Barrett JS. Population pharmacokinetic studies in pediatrics: issues in design and analysis. *AAPS J.* 2005;7(2):E475–87.
 58. Tod M, Jullien V, Pons G. Facilitation of drug evaluation in children by population methods and modelling. *Clin Pharmacokinet.* 2008;47(4):231–43.
 59. Chen N, Aleksa K, Woodland C, Rieder M, Koren G. Ontogeny of drug elimination by the human kidney. *Pediatr Nephrol.* 2006;21(2):160–8.
 60. Edgington AN, Schmitt W, Voith B, Willmann S. A mechanistic approach for the scaling of clearance in children. *Clin Pharmacokinet.* 2006;45(7):683–704.
 61. Johnson TN, Rostami-Hodjegan A, Tucker GT. Prediction of the clearance of eleven drugs and associated variability in neonates, infants and children. *Clin Pharmacokinet.* 2006;45(9):931–56.
 62. Edgington AN, Schmitt W, Willmann S. Development and evaluation of a generic physiologically based pharmacokinetic model for children. *Clin Pharmacokinet.* 2006;45(10):1013–34.
 63. Alcorn J, McNamara PJ. Ontogeny of hepatic and renal systemic clearance pathways in infants part I. *Clin Pharmacokinet.* 2002;41(12):959–98.
 64. Alcorn J, McNamara PJ. Ontogeny of hepatic and renal systemic clearance pathways in infants: part II. *Clin Pharmacokinet.* 2002;41(13):1077–94.
 65. Allegaert K, van den Anker JN, Naulaers G, de Hoon J. Determinants of drug metabolism in early neonatal life. *Curr Clin Pharmacol.* 2007;2(1):23–9.

66. Anderson GD (2010) Developmental pharmacokinetics. *Seminars in Pediatric Neurology*, (Elsevier), pp 208-213.
67. Hines RN, McCarver DG. The ontogeny of human drug-metabolizing enzymes: phase I oxidative enzymes. *J Pharmacol Exp Ther*. 2002;300(2):355–60.
68. McCarver DG, Hines RN. The ontogeny of human drug-metabolizing enzymes: phase II conjugation enzymes and regulatory mechanisms. *J Pharmacol Exp Ther*. 2002;300(2):361–6.
69. Holliday M, Potter D, Jarrah A, Bearg S. The relation of metabolic rate to body weight and organ size. *Pediatr Res*. 1967;1(3):185–95.
70. Wang C, Sadhavisvam S, Krekels EH, Dahan A, Tibboel D, Danhof M, Vinks AA, Knibbe CA. Developmental changes in morphine clearance across the entire paediatric age range are best described by a bodyweight-dependent exponent model. *Clinical Drug Investigation*. 2013;33(7):523–34.
71. Bartelink I, Boelens JJ, Bredius RG, Egberts AC, Wang C, Bierings MB, Shaw PJ, Nath CE, Hempel G, Zwaveling J. Body weight-dependent pharmacokinetics of busulfan in paediatric haematopoietic stem cell transplantation patients. *Clin Pharmacokinet*. 2012;51(5):331–45.
72. Mahmood I, Tegenge M. A bodyweight-dependent allometric exponent model for scaling clearance of clotting factor VIII and IX from infants to adults. *Haemophilia*. 2016;22(6):e570–3.
73. Mahmood I, Tegenge MA. A comparative study between allometric scaling and physiologically based pharmacokinetic modeling for the prediction of drug clearance from neonates to adolescents. *J Clin Pharmacol*. 2019;59(2):189–97.
74. Holford N. Dosing in children. *Clinical Pharmacology & Therapeutics*. 2010;87(3):367–70.
75. Mahmood I. Dosing in children: a critical review of the pharmacokinetic allometric scaling and modelling approaches in paediatric drug development and clinical settings. *Clin Pharmacokinet*. 2014;53(4):327–46.
76. Barrett JS, Barrett RF, Vinks AA. Status toward the implementation of precision dosing in children. *J Clin Pharmacol*. 2021;61:S36–51.
77. Anderson BJ, Holford NH. Understanding dosing: children are small adults, neonates are immature children. *Arch Dis Child*. 2013;98(9):737–44.
78. Jotterand Chaparro C, Moullet C, Taffé P, Laure Depeyre J, Perez MH, Longchamp D, Cotting J. Estimation of resting energy expenditure using predictive equations in critically ill children: results of a systematic review. *J Parenter Enter Nutr*. 2018;42(6):976–86.
79. Müller MJ, Geisler C, Hübers M, Pourhassan M, Braun W, Bosy-Westphal A. Normalizing resting energy expenditure across the life course in humans: challenges and hopes. *Eur J Clin Nutr*. 2018;72(5):628–37.
80. Fuentes-Servín J, Avila-Nava A, González-Salazar LE, Pérez-González OA, Servín-Rodas MDC, Serralde-Zuñiga AE, Medina-Vera I, & Guevara-Cruz M (2021) Resting energy expenditure prediction equations in the pediatric population: a systematic review. *Frontiers in Pediatrics* 9.

Publisher's Note Springer Nature remains neutral with regard to jurisdictional claims in published maps and institutional affiliations.